

Table S1. Primers used in this study. Related to STAR METHODS.

No.	Name	Sequence
1	Ecoli_dnaK_fow	GAGGCTCACAGAGAACAGATTGGTGGGATGGGTAAAAT AATTGGTATCG
2	Ecoli_dnaK_rev	CTTTCGGGCTTTGTTAGCAGCCGGATCAGTTATTTTTTGT CTTTGACTTCTTCAAATTC
3	Ecoli_dnaJ_fow	GAGGCTCACAGAGAACAGATTGGTGGGATGGCTAAGCA AGATTATTACG
4	Ecoli_dnaJ_rev	CTTTCGGGCTTTGTTAGCAGCCGGATCAGTTAGCGGG TCAGGTCGTCAAAAACTTC
5	Ecoli_grpE_fow2	GAGGCTCACAGAGAACAGATTGGTGGGATGAGTAGTAAAGA ACAGAAAACGCCTGAGGGGCAAG
6	Ecoli_grpE_rev2	CTTTCGGGCTTTGTTAGCAGCCGGATCAGTTAAGCTTTTGC TTTCGCTACAGTAACCATCGCC
7	pETS_Mtb_dnaK_NBD_fwd	CCGGCGTCCTCAAGGGCGAGTGACTGATCCGGCTGCTAAC
8	pETS_Mtb_dnaK_NBD_rev	GTTAGCAGCCGGATCAGTCACTCGCCCTTGAGGACGCCGG
9	pETS_Mtb_dnaK_SBD_fwd	ACAGAGAACAGATTGGTGGGGTCAAAGACGTTCTGCTGCT
10	pETS_Mtb_dnaK_SBD_rev	AGCAGCAGAACGTCTTTCACCCCAACCAATCTGTTCTCTGT
11	Mtb_dnaK_R127A_fwd	TTCAATGACGCCAGGCGCAGGCCACCAAGG
12	Mtb_dnaK_R127A_rev	CCTTGGTGGCCTGCGCCTGGGCGTCATTGAA
13	Mtb_dnaK_E398A_fwd	CCCACCAAGCGGTTCGGCCACTTTCACCAC
14	Mtb_dnaK_E398A_rev	GTGGTGAAAGTGGCCGACCGCTTGGTGGG CCAAGCGGTTCGGAGACTGCCACCACCGCCGACGACAAC
15	Mtb_dnaK_F400A_fwd	CAACC GGTTGGTTGTCGTTCGGCGGTGGTGGCAGTCTCCGACCGCT
16	Mtb_dnaK_F400A_rev	TGG CCAAGCGGTTCGGAGACTTTCGCCACCAGCCGACGACAACCAA
17	Mtb_dnaK_T401A_fwd	CC GGTTGGTTGTCGTTCGGCGGTGGCGAAAGTCTCCGACCGCTT
18	Mtb_dnaK_T401A_rev	GG
19	Mtb_dnaK_D404A_fwd	ACTTCACCACCGCCGCGGACAACCAACG
20	Mtb_dnaK_D404A_rev	CGTTGGTTGTCGGCGGCGGTGGTGAAGT
21	Mtb_dnaK_N406A_fwd	CGACGACGCCCAACCGTTCGGTGCAGATCCAGG
22	Mtb_dnaK_N406A_rev	CCTGGATCTGCACCGACGGTTGGGCGTTCGTCG
23	Mtb_dnaK_E514A_fwd	CGTAATCAAGCCGCCACATTGGTCTACCAG
24	Mtb_dnaK_E514A_rev	CTGGTAGACCAATGTGGCAGGCTTGATTACG GAGGCTCACAGAGAACAGATTGGTGGGATGTCCAAGG
25	pETHisSUMO_Hsc70_fow	GACCTGCAGTTGGTAT CTTTCGGGCTTTGTTAGCAGCCGGATCAGTTAATCAACCT
26	pETHisSUMO_Hsc70_rev	CTTCAATGGTGGG GAGGCTCACAGAGAACAGATTGGTGGGATGGCTAACGTGG
27	pETHisSUMO_Hsdnaja2_fow	CTGACACGAAG
28	pETHisSUMO_Hsdnaja2_rev	CTTTCGGGCTTTGTTAGCAGCCGGATCAGTTACTGATGG GCACACTGCACTC

Table S1. Primers used in this study, continued. Related to STAR METHODS.

No.	Name	Sequence
29	oAF674	GAATCTAGAATCGAGGAGTGGGTG
30	oAF675	GTAGAATTCTCACTTGGCCTCCCG

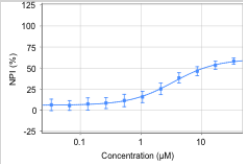
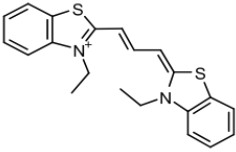
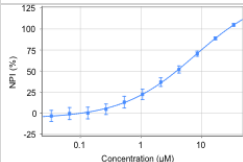
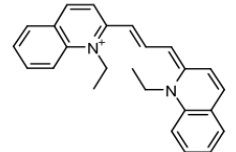
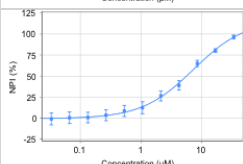
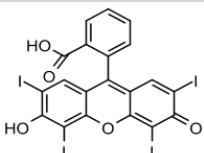
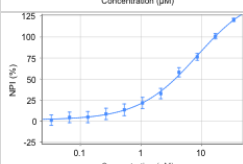
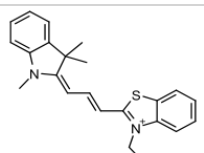
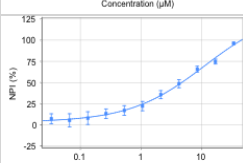
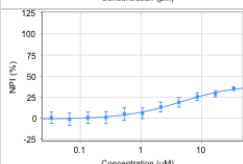
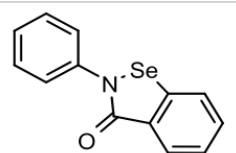
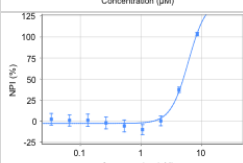
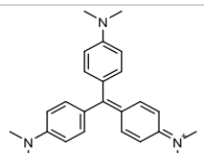
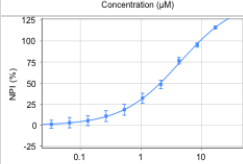
Table S2. Plasmids used in this study. Related to STAR METHODS.

No.	Plasmid name	Description	Source
1	pETHisSUMO	pET His6 Sumo TEV LIC cloning vector (Amp ^R)	Addgene #29711
2	pHYRS52	His6-S. cerevisiae ulp1 (res. 403-621) (Amp ^R)	Addgene #31122
3	pET-47b(+)	N-terminal His6 (Kan ^R)	Novagen
4	BMN146	pETHis6 SUMO Mtb DnaK R127A;	This work
5	SD9	pETHis6 SUMO DnaK parent, primers 11+12	Lupoli et al., 2016
6	JTH100	pETHis6 SUMO Mtb DnaK T175A	This work
7	JTH126	pETHis6 SUMO Mtb DnaK NBD T175A (res. 1-359);	This work
8	JTH265	pETHis6 SUMO DnaK T175A parent, primers 7+8	This work
9	JTH266	pET His6 SUMO Mtb DnaK SBD (res. 360-625),	This work
10	JTH267	pETHis6 SUMO DnaK parent, primers 9+10	This work
11	JTH268	pETHis6 SUMO Mtb DnaK E398A;	This work
12	JTH269	pETHis6 SUMO DnaK parent, primers 13+14	This work
13	JTH271	pETHis6 SUMO Mtb DnaK F400A;	This work
14	AR135	pETHis6 SUMO DnaK parent, primers 15+16	This work
15	AR136	pETHis6 SUMO Mtb DnaK T401A;	This work
16	AR137	pETHis6 SUMO DnaK parent, primers 17+18	This work
17	TL144	pETHis6 SUMO Mtb DnaK D404A;	This work
18	TL145	pETHis6 SUMO DnaK parent, primers 19+20	This work
19	TL03	pETHis6 SUMO Mtb DnaK N406A;	This work
20	TL04	pETHis6 SUMO DnaK parent, primers 21+22	This work
21	TL05	pETHis6 SUMO Mtb DnaK E514A;	This work
22	TL06	pETHis6 SUMO DnaK parent, primers 23+24	This work
23	pcDNA5/FRT/TO HIS HSPA8	pET His6 SUMO <i>E. coli</i> DnaK	This work
24	pcDNA5/FRT/TO DNAJA2	pET His6 SUMO, MG1655 template, primers 1+2	This work
25	pAJF465	pET His6 SUMO <i>E. coli</i> DnaJ	This work
26	pDB60	pET His6 SUMO, MG1655 template, primers 3+4	This work
		pET His6 SUMO <i>E. coli</i> GrpE	This work
		pET His6 SUMO, MG1655 template, primers 5+6	This work
		pET His6 SUMO human Hsc73 (HspA8);	This work
		pET His6 SUMO, plasmid 23 template, primers 25+26	This work
		pET His6 SUMO DnaJA2;	This work
		pET His6 SUMO, plasmid 24 template, primers 27+28	This work
		His6-SUMO-Mtb DnaJ1	Lupoli et al., 2016
		His6-SUMO-Mtb DnaJ2	Lupoli et al., 2016
		His6-SUMO-Mtb GrpE	Lupoli et al., 2016
		His6-SUMO-Mtb DnaK	Lupoli et al., 2016
		Human Hsc70 cloning vector	Addgene #19541
		Human DnaJA2 cloning vector	Addgene #19465
		<i>attB</i> ::Mtb <i>dnaK</i> (Strep ^R)*	This work
		Complementation vector (Strep ^R , <i>attP</i> (L5))	Glickman lab

Table S3. Strains used in this study. Related to STAR METHODS.

No.	Strain name	Description	Source
1	Rosetta2 (DE3)	<i>E. coli</i> BL21 derivative for rare codon usage	Novagen
2	Rosetta2 (DE3) pLysS	Rosetta2 expressing T7 lysozyme	Novagen
3	EcTL03	Rosetta2 expressing His6-SUMO-Mtb DnaJ1	Lupoli et al., 2016
4	EcTL04	Rosetta2 expressing His6-SUMO-Mtb DnaJ2	Lupoli et al., 2016
5	EcTL05	Rosetta2 expressing His6-SUMO-Mtb GrpE	Lupoli et al., 2016
6	EcTL06	Rosetta2 expressing His6-SUMO-Mtb DnaK	Lupoli et al., 2016
7	His6 SUMO-Mtb DnaK NBD and full-length mutants	Rosetta2 transformed with a single plasmid (4-6)	This work
8	His6 SUMO-Mtb DnaK SBD and full-length mutants	Rosetta2(De3) pLysS transformed with a single plasmid (7-13)	This work
9	His6 SUMO <i>E. coli</i> DnaK	Rosetta2 expressing His6-SUMO- <i>E. coli</i> DnaK	This work
10	His6 SUMO <i>E. coli</i> DnaJ	Rosetta2 expressing His6-SUMO- <i>E. coli</i> DnaJ	This work
11	His6 SUMO <i>E. coli</i> GrpE	Rosetta2 expressing His6-SUMO- <i>E. coli</i> GrpE	This work
12	His6 SUMO Hsc73	Rosetta2 expressing His6-SUMO-Hsc73	This work
13	His6 SUMO DnaJA2	Rosetta2 pLys expressing His6-SUMO-DnaJA2	This work
14	mc ² 155	<i>M. smegmatis</i> wild-type	Gift of Glickman lab
15	MGM6069	<i>M. smegmatis</i> Δ <i>dnaj1 attB::strep</i> ^R	Lupoli et al, 2016
16	MGM6031	<i>M. smegmatis</i> Δ <i>dnaj2::loxP</i>	Lupoli et al, 2016
17	MGM6003	<i>M. smegmatis</i> Δ <i>dnaK attB::dnaK-mCitrine Kan</i> ^R	Fay & Glickman, 2014
18	MGM6933	<i>M. smegmatis</i> Δ <i>dnaK attB::Mtb dnaK</i> (Strep ^R) (MGM6003 transformed with pAJF465)	This work

Table S4. Initial hits from “drug repurposing” library.* Related to Figures 1 and S1.

Molecule ID	Structure	initial IC ₅₀ (μM)	Dose-Response Plot	HPLC Purity (%)
RU-0423251	Telaprevir (TP)	3.42		91.2
RU-0187364		7.75		100
RU-0187363		7.41		100
RU-0162152		8.52		95.3
RU-0084237		11.4		100
RU-0084126	2Cl-B-MECA (MECA)	4.56		98
RU-0024306		6.07		100
RU-0000160		4.42		90.4

* Structure IDs, chemical structures, initial IC₅₀ values determined by plate-format ATPase assay; compound purity determined by HPLC. Note that RU-0000160 is the common dye crystal violet.

Table S5. Initial hits from the “drug-like” library.* Related to Figures 1 and S1.

Molecule ID	Structure	initial IC50 (μM)	Dose-Response Plot	HPLC Purity (%)
RU-0278796		9.59		100
RU-0272931		11.4		96.5
RU-0415073		11.8		100
RU-0201380		13		100
RU-0272639		14.4		100
RU-0274435		17.1		100
RU-0272753		17.4		96.5
RU-0275942		20.1		100
RU-0277166		21.5		100
RU-0274544		> 34.0		97

* Structure IDs, chemical structures, initial IC50 values determined by plate-format ATPase assay; compound purity determined by HPLC.

Table S6. Summary of residues that were identified as sites of covalent modification by probe 7 in Mtb DnaK SBD after digestion followed by electrospray MS/MS. Related to Figures 5 and S5.

RESIDUE	CSMs ^A	CORRESPONDING PEPTIDE(S)
L365	1	.VKDVLL[+530.284]LDVTPLSLGIETK.G
K395	2	R.NTTIPTK[+530.284]R.S
E398	20	R.SE[+530.284]TFTTADDNQPSVQIQVYQGER.E
T399	1	R.SET[+530.284]FTTADDNQPSVQIQVYQGER.E
A403	1	R.SETFTTA[+530.284]DDNQPSVQIQVYQGER.E
D405	7	R.SETFTTADD[+530.284]NQPSVQIQVYQGER.E
N406	25	R.SETFTTADDN[+530.284]QPSVQIQVYQGER.E, R.SETFTTADDN[+530.284]QPSVQIQ[+0.984]VYQGER.E
S409	2	K.RSETFTTADDNQPS[+530.284]VQIQVYQGER.E
Y415	1	K.RSETFTTADDNQPSVQIQVY[+530.284]QGER.E
H424	1	R.EIAAH[+530.284]NK.L
N425	2	R.EIAAHN[+530.284]K.L
S482	2	R.IQEGSGLS[+530.284]KEDIDR.M
E494	1	K.DAE[+530.284]AHAEEDR.K
H496	1	R.M[+15.995]IKDAEAH[+530.284]AEEDR.K
E499	1	K.DAEAHAE[+530.284]DR.K
Y518	1	R.NQAETLVY[+530.284]QTEK.F
E538	3	R.EAEGGSKVPE[+530.284]DTLNKVDAAVAEAK.A
T540	4	R.EAEGGSKVPEDT[+530.284]LNKVDAAVAEAK.A
N542	1	R.EAEGGSKVPEDTLN[+530.284]KVDAAVAEAK.A

^a Color coding corresponds to residues shown in **Figure S5**.

Table S7. MIC₅₀ values for indicated strains with aminoglycosides in the presence and absence of telaprevir (TP) in 1% total DMSO.^a Related to Figures 7 and S7.

Strain	Streptomycin ($\mu\text{g/mL}$)		Kanamycin ($\mu\text{g/mL}$)	
	+ TP (100 μM)	DMSO	+ TP (100 μM)	DMSO
Msm WT	0.0216 (0.0135)	0.0958 (0.0254)	0.193 (0.0435)	0.337 (0.0759)
Msm ΔdnaJ1	N/A ^b	N/A ^c	N/A	0.311 (0.0951)
Msm ΔdnaJ2	0.0300 (.00819)	0.0907 (0.0186)	0.268 (0.0521)	0.356 (0.188)

^a MIC₅₀ values are an average of three independent experiments performed in triplicate. Standard deviation (SD) of n=3 triplicate experiments shown in parentheses.

^b N/A = not applicable. Growth of Msm ΔdnaJ1 cells is inhibited by 100 μM TP as shown in **Figure S7F**.

^c This strain is resistant to streptomycin and so an MIC₅₀ value was not determined.

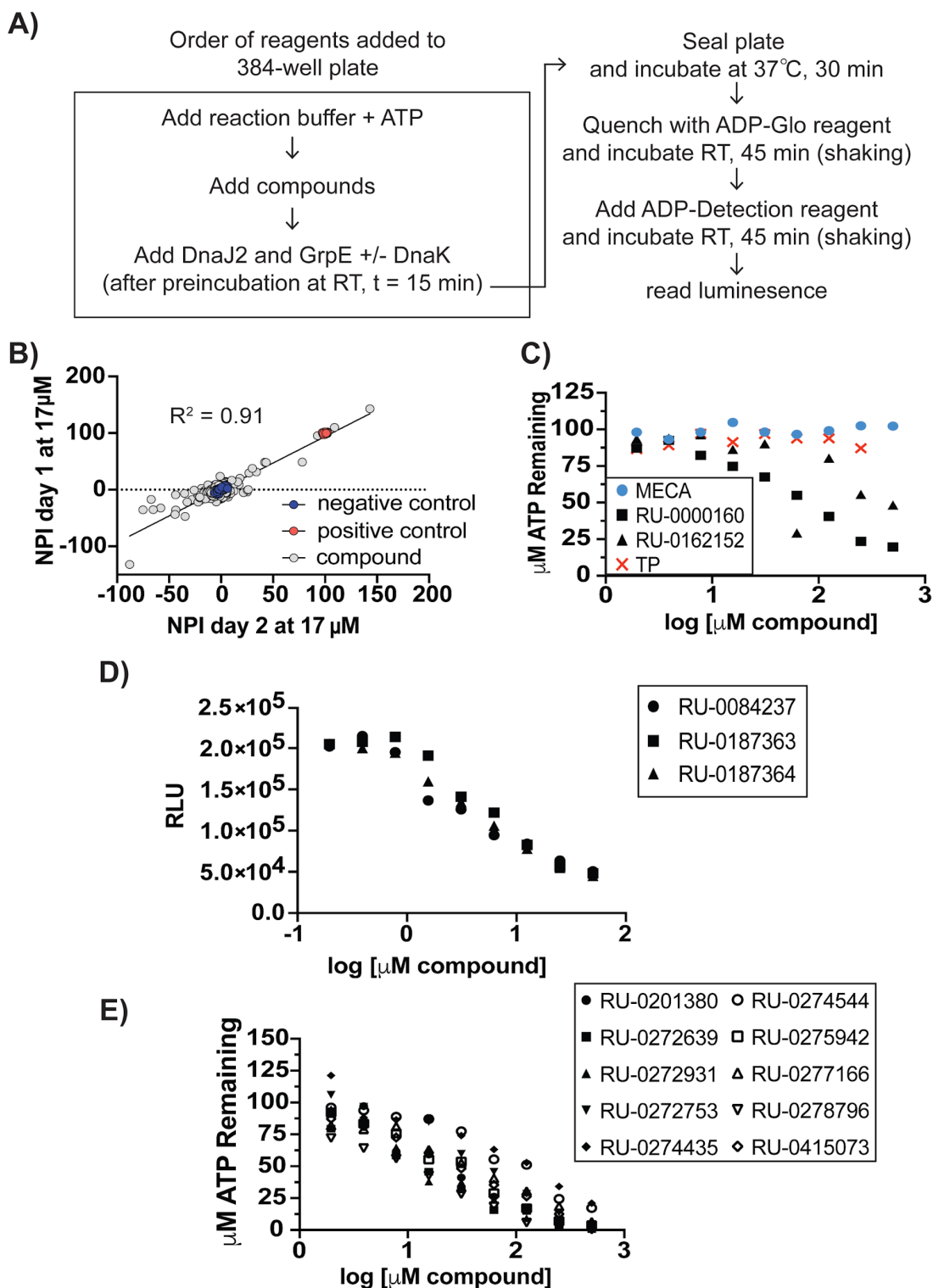


Figure S1. Overview of high-throughput screen and assessment of hits for luciferase inhibition. (A) Schematic of protocol for high-throughput screening approach entailing a coupled luciferase-dependent assay. See the Methods for a detailed description of the screen set-up. (B) Comparison of pilot library results over two consecutive days (NPI = normalized product inhibition) with a hit rate of 0.9%. (C) Luciferase activity in the presence of select “drug-repurposing” library hits including TP and MECA. TP and

MECA do not inhibit luciferase at indicated concentrations, while aromatic compounds RU-0000160 and RU-0162152 show inhibition. (D) Structurally similar compounds from the “drug repurposing” library all show similar inhibition profiles against luciferase. Higher RLU values correlate to higher ATP concentrations detected. (E) All ten compound hits from the “drug-like” library disrupt luciferase activity. For C-E, assay setup was performed as described for ATPase assays in the Methods, except DnaK and cofactors were not included in the reactions (t = 30 min). Note that RU-0024306 was not tested due to limited compound stock and because the scaffold is not ideal for targeted protein inhibition in cells. Related to **Figure 2** and **Tables S4** and **S5**.

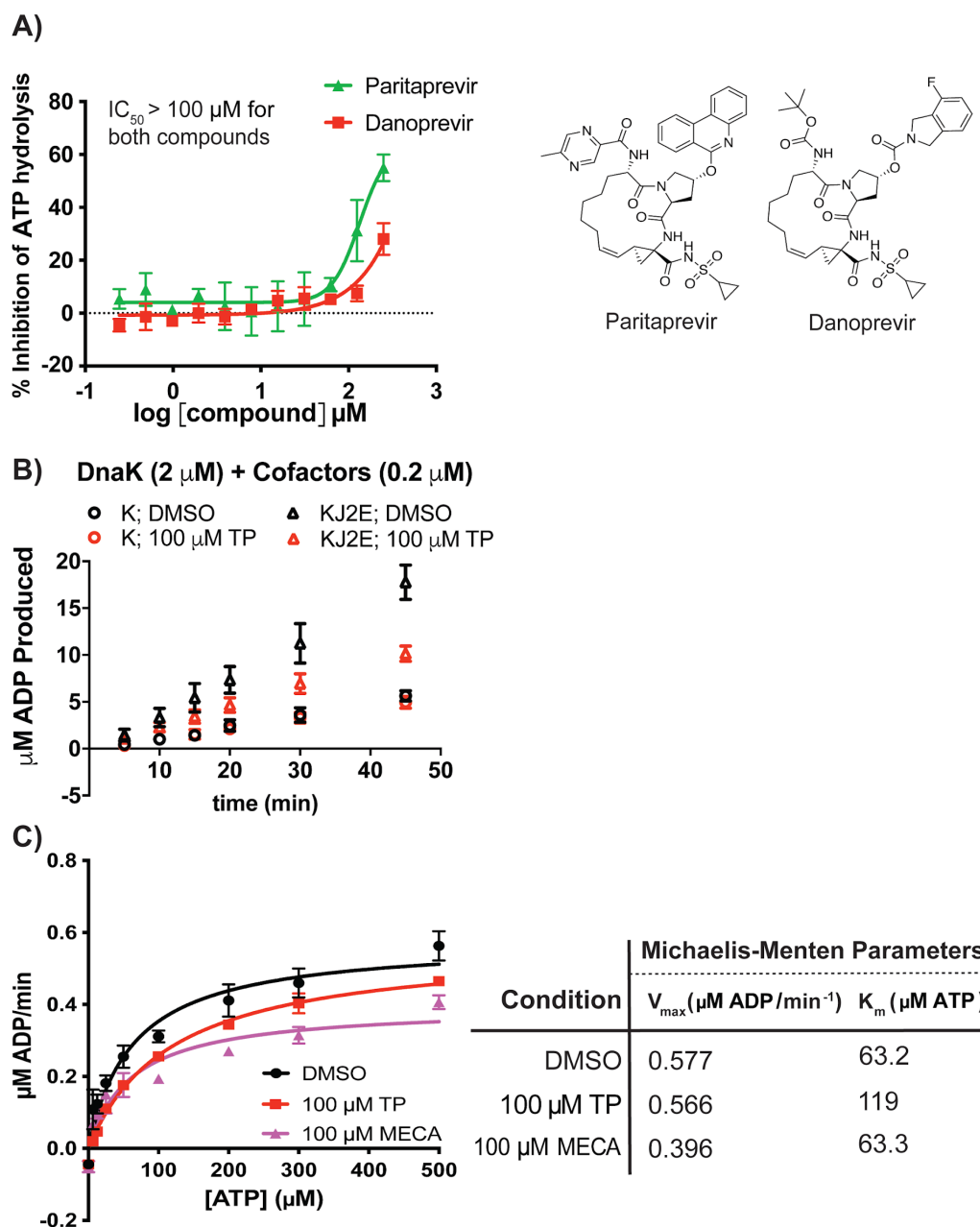


Figure S2. ATPase assays indicate allosteric mechanisms of DnaK and cofactor inhibition by select small molecules. (A) Dose-response assays indicate that additional HCV protease inhibitors (structures shown) are not potent Mtb DnaK ATPase inhibitors. Addition of varying concentrations of indicated compounds to Mtb DnaK-DnaJ2-GrpE shows inhibition only at high concentrations. IC₅₀ experiments were conducted using assay conditions described in the Methods section. (B) TP inhibits activation of DnaK by cofactor proteins. Time course of Mtb DnaK alone and with DnaJ2 and GrpE in the presence and absence of telaprevir (100 μM) shows disruption of DnaK ATPase activation by cofactors but not DnaK alone. (C) Michaelis-Menten kinetic analyses indicate that TP increases the K_m of the DnaK-DnaJ2-GrpE reaction, while MECA decreases the V_{max} . Mtb DnaK was first incubated with 100 μM drug, then 0.2 μM DnaJ2 and GrpE were added, followed by initiation with varying [ATP]. Reactions were quenched at 20 min. This data

suggests that TP affects binding of ATP in the NBD, while MECA does not (MECA acts as a non-competitive inhibitor). For all experiments, $n = 3$, and error bars indicate standard deviation (SD). Related to **Figure 2**.

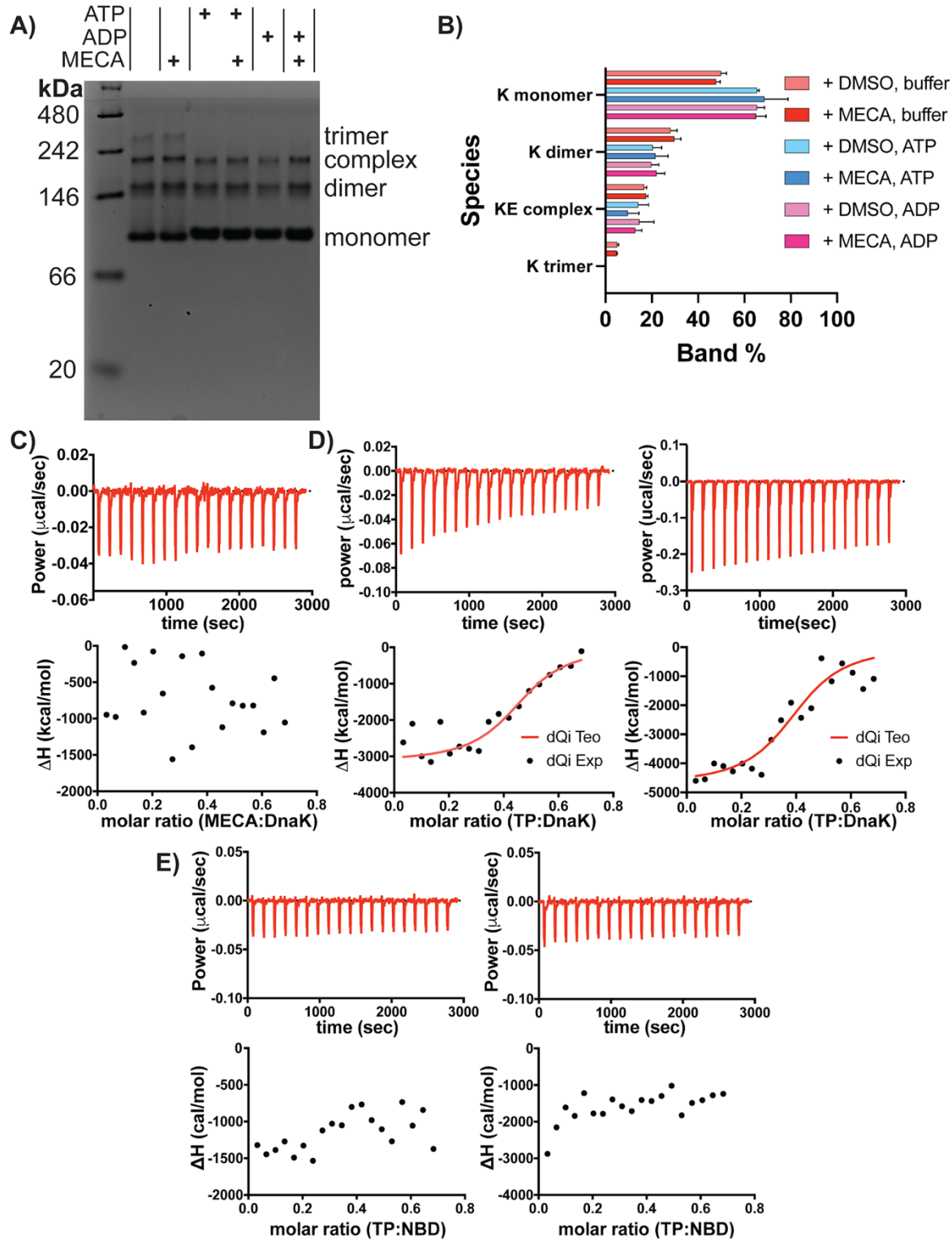


Figure S3. Analyses of interactions between DnaK and small molecules indicates that TP binds directly to DnaK, while MECA does not. (A) Native gel electrophoresis analysis of DnaK/GrpE complex formation in the presence and absence of nucleotides with and without MECA (100 μ M) added. (B) Quantification of the relative abundance of each band from replicate experiments of the gel shown in part A shows no significant difference in formation of any species upon addition of excess MECA ($n = 3$, error bars indicate SD). See Methods for detailed protocol. (C) ITC analysis of full-length apo DnaK T175A with MECA reveals a lack of binding to DnaK T175A alone. Replicate ITC experiments for TP binding in the presence of (D) full-length apo DnaK T175A and (E) the nucleotide binding domain (NBD) of apo DnaK T175A. TP binds to full-length DnaK, but not the NBD truncation. Related to **Figure 4**.

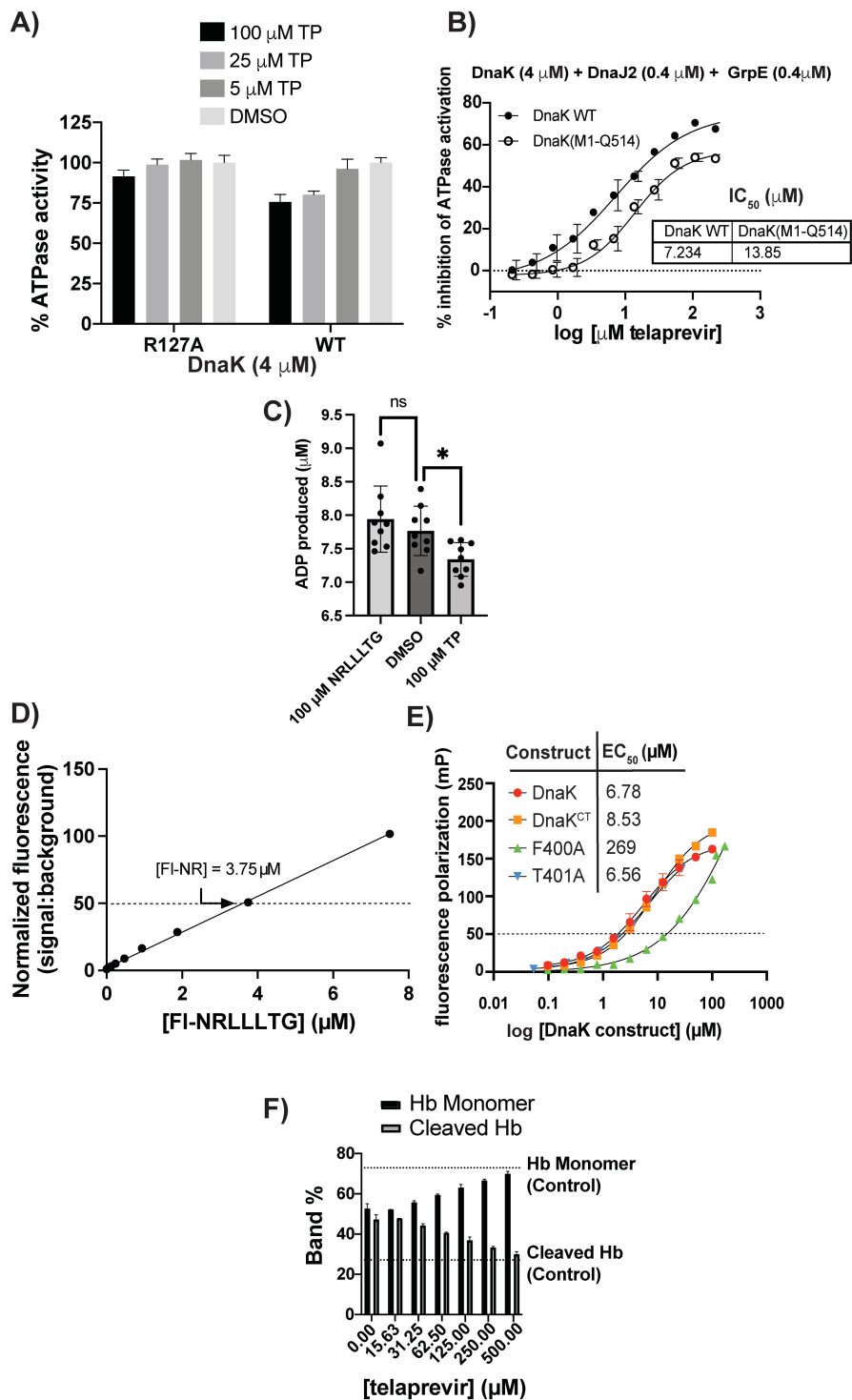


Figure S4. TP binds to the beta-sandwich subdomain of the substrate binding domain (SBD) of DnaK. (A) ATPase analysis of DnaK wild-type and R127A treated with decreasing concentrations of TP (t = 30 min). At high concentrations of TP, there is a small decrease in ATP turnover by WT DnaK but not

R127A, which is a mutation that disrupts allosteric communication between the NBD and SBD of DnaK. These data suggest that TP requires allosteric communication between the two domains to inhibit ATPase activity in the NBD. (n = 3, error bars indicate SD) (B) DnaK (M1-Q512) was titrated with TP and showed similar IC₅₀ values to wild-type under the same experimental conditions (t = 30 min), suggesting that the C-terminus of the alpha-helical domain is not required for inhibition. (n = 3, error bars indicate SD). (C) ADP produced by DnaK (4 μM) incubated with indicated concentrations of NRLLLTG or TP and compared to vehicle-only (DMSO) for t = 30 min (n = 9, error bars indicate SD). *p < 0.05, unpaired t-test was used for comparison of indicated data points; ns: non-significant). For all ATPase assays, activity was assessed as described in Methods. Fluorescence polarization (FP) assay optimization was performed by carrying out the following experiments: (D) determination of [FL-NRLLLTG] at which fluorescence signal:noise exceeds 50 ([FL-NR] = 3.75 μM) and (E) determination of a [DnaK] at which fluorescence polarization signal exceeds 100 mP (Rossi and Taylor, 2011; Moerke, 2009). Selected concentrations were then used for displacement assays with other compounds. Representative singleton experiments are shown. F) Digestion of the model substrate hemoglobin (Hb) with proteinase K in the presence of increasing concentrations of TP after quantification of band intensities following SDS-PAGE analysis. The dashed lines indicate percentages of Hb monomer and proteolysis products when no proteinase K was added (control). Note that 50 μM TP is not anticipated to inhibit proteinase K cleavage activity. Related to **Figure 4**.

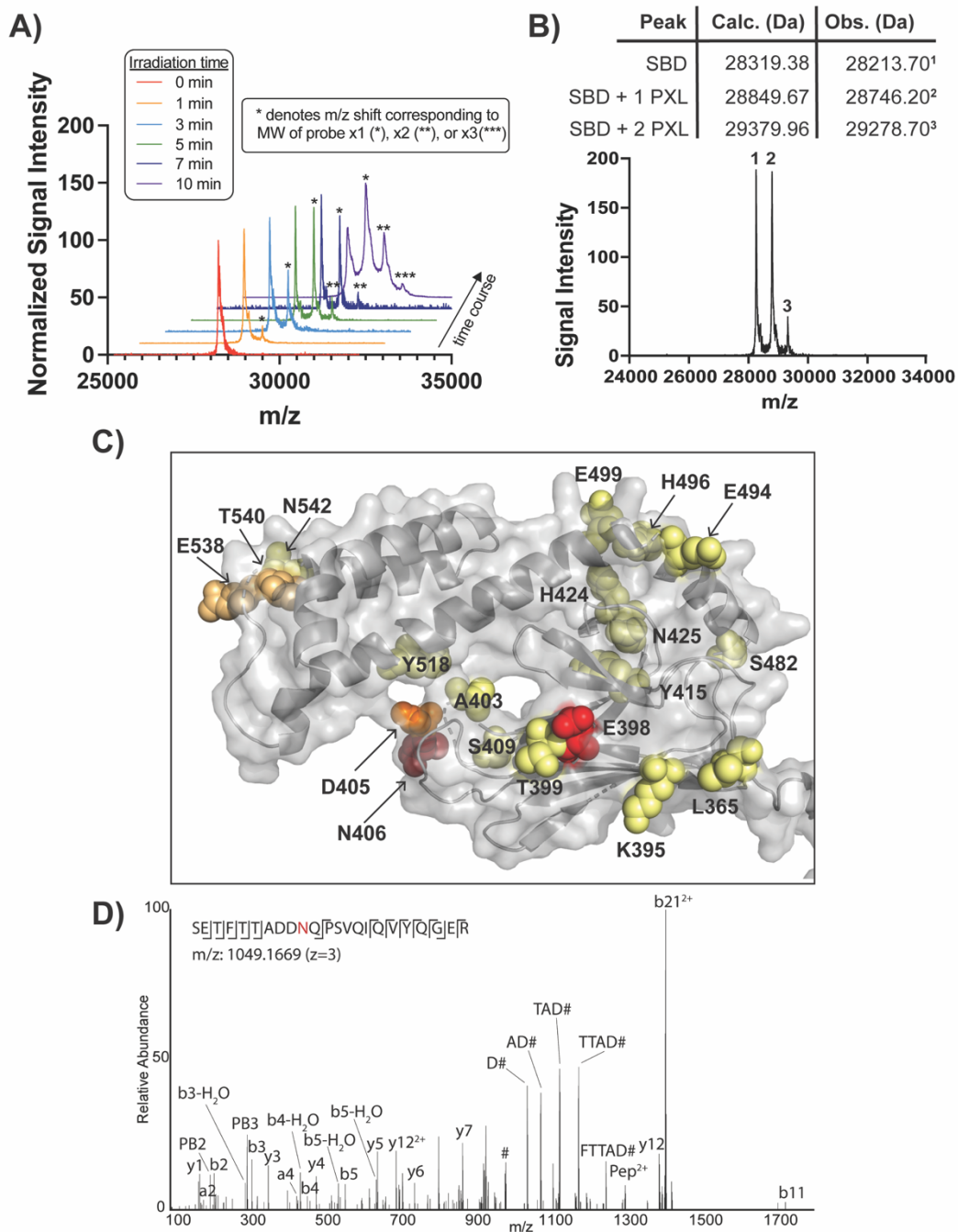


Figure S5. Photo-crosslinking optimization and mass spectrometry (MS) analyses demonstrate crosslinking of 7 to the peptide binding subdomain of the SBD. (A) A time course experiment was conducted to find the optimal time point for crosslinking of 7 to DnaK. Each MALDI-TOF trace indicates a different irradiation time and the number of molecules of peptide 7 that is crosslinked to DnaK is indicated. (B) Covalent modification at $t = 5$ min, at which time an approximately 50:50 signal of the single modified (+532.5001 Da adduct) and unmodified protein can be detected, with minimal non-specific crosslinking product resulting from crosslinks to two 7 peptides (+1065.001 peak). The expected mass increase for covalent modification is 530.285 Da; although the accuracy of the available MALDI-TOF for intact proteins is poor, it could still be used to assess relative quantities of crosslinked species (PXL = photo-crosslink).

(C) Visual representation of residues that were identified as sites of covalent modification by probe 7 in Mtb DnaK SBD by digestion followed by electrospray MS/MS. Color coding corresponds to the number of crosslink spectral matches (CSMs) at each residue, as detailed in **Table S6**. (D) Shown here is the Higher-Energy Collision Dissociation (HCD) MS/MS spectrum ($(M + 3H)^{+3}$ ions) of SETFTTADDNQPSVQIQVYQGER (one of the most highly modified peptides) acquired on an Orbitrap Eclipse Tribrid with 30,000 resolution (@ 400 m/z). N-terminal fragment ions (b-type ions) are indicated by] and C-terminal fragment ions (y-type ions) are indicated by [. Doubly charged ions are indicated with 2+. The red character indicates the likely placement of the probe modification within the sequence. PB2 and PB3 indicate fragment ions of the probe 206.093 and 305.161 Da respectively. # indicates the internal fragment ion containing peptide DNQPSVQIQVYQG and N-terminal additional amino acids as indicated (e.g. D# is DDNQPSVQIQVYQG). Related to **Figure 5, Table S6**.



Figure S6. Alignment of substrate binding domains of DnaKs and Hsp70s with important residues in peptide binding domain highlighted. Alignment of SBDs of Hsp70 family members from humans, yeast and multiple prokaryotes (DnaKs). Secondary structure-based labeling was obtained from previous work on *E. coli* DnaK (Zhu *et al.*, 1996). Peptide binding site residues were highlighted for human (blue) and prokaryotes (yellow) (Chiappori *et al.*, 2015). Refer to key for color-coding of important residues. Alignment was performed using Clustal Omega. Related to **Figure 6**.

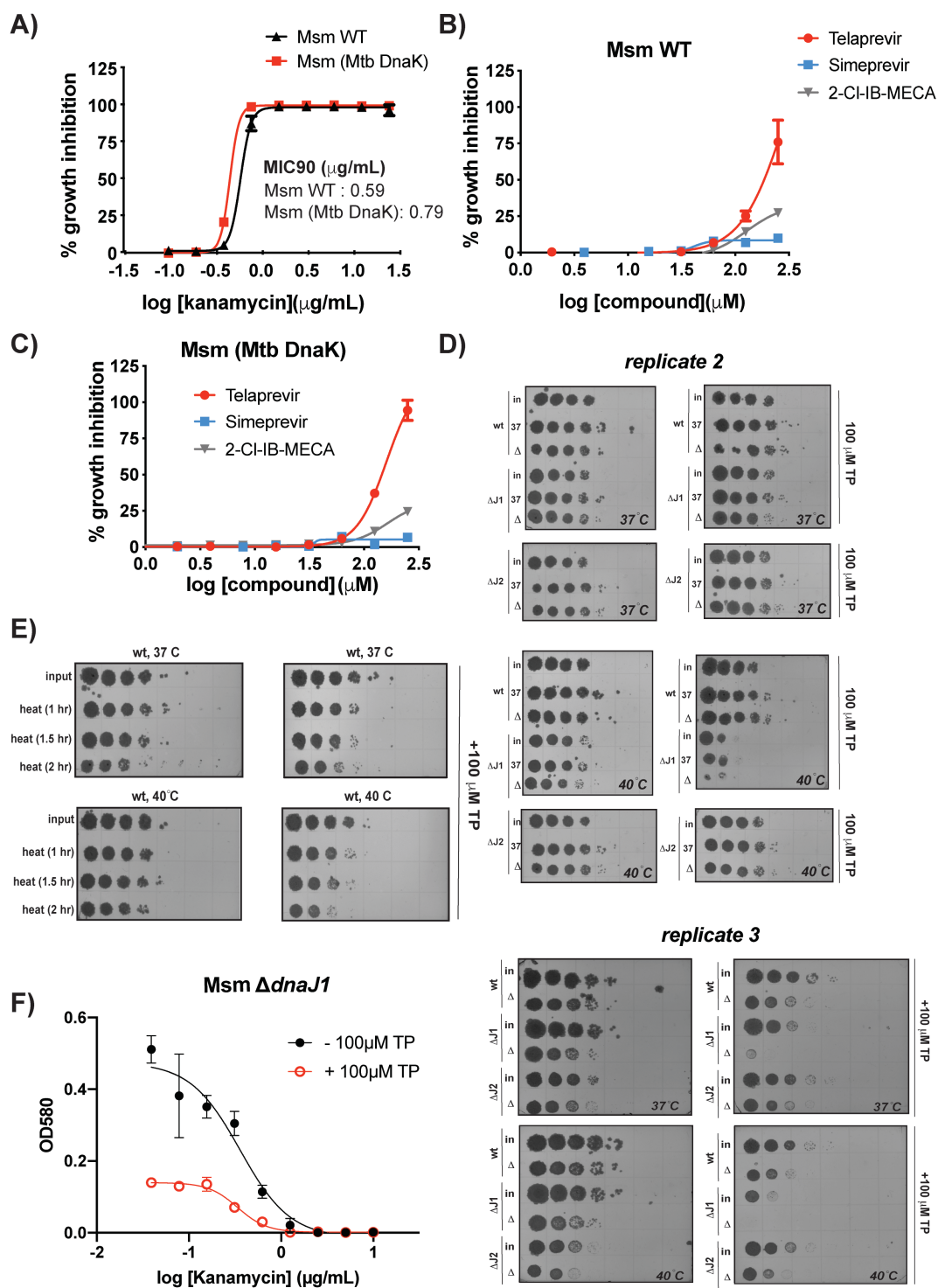


Figure S7. Cell-based assays using *Mycobacterium smegmatis* (Msm) indicate high concentrations of TP inhibit recovery after cells are exposed to prolonged heat stress. (A) Both Msm wild-type and MGM6933 (Msm $\Delta dnaK$ expressing Mtb *dnaK*) cells show similar minimum inhibitory concentrations for 90% growth inhibition (MIC90s) with the known antibiotic kanamycin. Msm DnaK shares approximately 89% sequence identity with its homolog in Mtb. (B) Msm wild-type shows sensitivity to telaprevir only at

concentrations >100 μM ; similar concentrations of simeprevir and 2-Cl-IB-MECA do not affect growth. (C) MGM6933 cells behave similar to Msm wild-type in part B in the presence of indicated compounds. For dose response experiments, plates were read at $t = 2$ days, and growth was compared to wells containing vehicle only. (D) Replicates for heat shock assay shown in **Figure 7A**. Recovery of indicated Msm strains following heat shock (53 $^{\circ}\text{C}$, 1 hour) prior to growth +/- TP at 37 $^{\circ}\text{C}$ or 40 $^{\circ}\text{C}$ indicates that cells lacking *dnaJ1* are the most sensitive to TP following global protein denaturation. Cell dilution factor increases from left to right across each plate. Wt: Msm; $\Delta J1$: Msm $\Delta dnaJ1$; $\Delta J2$: Msm $\Delta dnaJ2$; Δ : heat; in: input. Note that in *replicate 2*, the rows labeled "37" indicate samples incubated at 37 $^{\circ}\text{C}$ for 1 hr instead of undergoing heat shock. (E) Heat shock of Msm wild-type cells over indicated time course shows that cells become sensitive to TP after prolonged heat treatment. As described in the Methods section, cells were incubated at 53 $^{\circ}\text{C}$ for time indicated (heat) prior to dilution and plating on 7H10 plates with and without TP, and incubation at 37 or 40 $^{\circ}\text{C}$. Compared to the input, cells that are heat shocked for 2 hr and incubated at elevated temperature show about a 2- \log_{10} growth recovery defect with TP added; cells incubated without TP do not show the same extent of growth recovery defect, even when grown at elevated temperatures. Cell dilution factor increases from left to right across each plate. (F) Growth of Msm $\Delta dnaJ1$ over a range of kanamycin concentrations in the presence and absence of TP shows that 100 μM TP inhibits cell growth. Optical density at 580 nm (OD580) shown on day = 3. Related to **Figure 7** and **Table S7**.